Macromolecules

Volume 36, Number 12 June 17, 2003

Communications to the Editor

Phase Behavior of Poly(methyl methacrylate)/Poly(vinylidene fluoride) Blends with and without High-Pressure CO_2

Teri A. Walker,[†] Yuri B. Melnichenko,[§] George D. Wignall,[§] and Richard J. Spontak*[,†,‡]

Departments of Chemical Engineering and Materials Science & Engineering, North Carolina State University, Raleigh, North Carolina 27695, and Condensed Matter Sciences, Oak Ridge National Laboratory, Oak Ridge, Tennessee 37831

Received February 11, 2003

Introduction. Blends composed of poly(methyl methacrylate) (PMMA) and poly(vinylidene fluoride) (PVDF) are of commercial interest due to their synergistic physical properties. These blends marry the chemical/flame resistance, toughness, and piezoelectric nature of PVDF[1,2] with the modulus, tensile strength, low smoke toxicity, and optical properties of PMMA[3] and likewise exhibit intriguing phase behavior. The intermolecular interactions that arise from the electric moments of the polymers, as well as from hydrogen bonding between the carbonyl oxygen of PMMA and the acidic hydrogens of PVDF,[4,5] are responsible for lower critical solution temperature (LCST) behavior at temperatures well above the normal melting point (T_m) of PVDF. Thus, the blends are completely miscible over a wide temperature window in the melt. They are also partially miscible, existing as amorphous media, over a broad composition range (up to ~50 wt % PVDF) at temperatures below T_m (extending to the solid state at temperatures below the glass transition temperature of the blend, $T_{g,mix}$). Under these conditions, the blends can be processed or used as macroscopically homogeneous materials with intermediate properties. This benefit has been exploited by Siripurapu et al.,[6] who report that miscible PMMA/PVDF blends yield well-defined microcellular foams upon exposure to supercritical CO_2, whereas heterogeneous blends, as well as PVDF alone, do not.

In addition to its LCST behavior at elevated temperatures, there is considerable evidence to indicate that this blend also exhibits upper critical solution temperature (UCST) behavior at temperatures below the T_m of PVDF. Inoue and co-workers[7] have demonstrated the existence of such behavior by annealing miscible PMMA/PVDF blends at temperatures above $T_{g,mix}$ and following the onset of phase separation. Their first report places the coexistence curve between 110 and 140 °C, whereas their subsequent study suggests that the phase boundary lies closer to 140 °C. Using electron spin resonance, Shimada et al.[8] have arrived at a similar conclusion, with the critical temperature (T_c) estimated to be ~100 °C. Grinsted and Koenig[9] and Papavoine et al.[10] have employed nuclear magnetic resonance techniques to show that miscible PMMA/PVDF blends undergo phase separation at temperatures in the solid state as well as in the melt. While the existence of UCST behavior has been established, the phase diagram for PMMA/PVDF blends remains ambiguous. Moreover, relatively little is known about how the phase behavior of this blend changes upon exposure to a compressible fluid, such as high-pressure CO_2, which can be used to improve rheological properties[6] for facilitated processing or modify phase behavior[11] for specific applications. In this work, we explore the effects of temperature and CO_2 pressure on the Flory−Huggins χ parameter and the phase behavior of PMMA/PVDF blends.

Experimental Section. a. Materials. The PVDF (with $\bar{M}_w$ and $\bar{M}_w/\bar{M}_n$ reported by the manufacturer to be 140 000 and 2.5−3.0, respectively) was supplied by Polysciences, Inc. (Warrington, PA), whereas perdeuterated (d_8) PMMA (with $\bar{M}_w$ = 58 500 and $\bar{M}_w/\bar{M}_n$ = 1.06) was purchased from Polymer Source, Inc. (Dorval, Quebec, Canada). Both materials were used as-received.

[†] Department of Chemical Engineering, North Carolina State University

[‡] Department of Materials Science & Engineering, North Carolina State University.

[§] Oak Ridge National Laboratory.

* To whom correspondence should be addressed. E-mail: rich_spontak@ncsu.edu.

10.1021/ma030103c CCC: $25.00
Published on Web 05/23/2003

Carbon dioxide with a purity of 99.8% was obtained from Air Liquide Co. (Augusta, GA) and used without further purification.

b. Methods. A miscible 55/45 d_8-PMMA/PVDF blend was prepared by first hand-mixing and then melt-pressing the homopolymer powders at 185 °C for about 2 min. The mold assembly was quenched under pressure by flowing cold tap water through the cooling coils of the platens, and the resultant plaque was removed from the mold, cut into pieces, stacked, and subsequently melt-pressed again according to the "baker's" procedure,[12] which was repeated 10 times. High-temperature and pressure small-angle neutron scattering (SANS) experiments were performed on the SANS facility at Oak Ridge National Laboratory. Two-dimensional isotropic scattering patterns were collapsed to one-dimensional $I(q)$ plots via radial averaging. Here, I is the absolute scattered intensity corrected for detector efficiency and calibrated with respect to a secondary standard,[13] and q is the scattering vector defined as $(4\pi/\lambda)\sin(\theta/2)$, where λ is the neutron wavelength (4.75 Å) and θ denotes the scattering angle. The thermal properties of the neat homopolymers, as well as of the blend before and after exposure to high-pressure CO_2 at ambient and elevated temperatures, were determined by differential scanning calorimetry (DSC) with a Seiko DSC220C SSC/5200 calorimeter operated under an inert N_2 atmosphere. Each specimen examined was cooled at 100 °C/min to −100 °C, where it was held for 10 min. It was then heated at 10 °C/min from −100 to 200 °C, after which the cycle was repeated a second time.

Results and Discussion. Figure 1a shows a series of SANS patterns collected from the 55/45 d_8-PMMA/PVDF blend at several temperatures in the melt (T_m = 168 °C for the PVDF employed in this study, according to DSC analysis). The data shown in this figure have been acquired at ambient pressure in the absence of CO_2. Scattering patterns obtained from the blend in the presence of 13.8 MPa of CO_2 appear indistinguishable and are not included for that reason. Values of the Flory−Huggins χ parameter have been extracted using the random phase approximation (RPA)[14] expressed as

$$\frac{1}{S(q)} = \frac{1}{v_A N_{n,A} \phi_A S(x_A)} + \frac{1}{v_B N_{n,B} \phi_B S(x_B)} - \frac{2\chi}{v_0} \quad (1)$$

Here, $S(q)$ is the structure factor equal to $k/I(q)$ (where k represents the neutron contrast factor), v_i corresponds to the volume of repeat unit i (i = A or B), $N_{n,i}$ is the number-average degree of polymerization of polymer i, ϕ_i denotes the volume fraction of polymer i in the blend, and v_0 is a reference volume ($v_0 = \sqrt{v_A v_B}$). For polydisperse polymers, each $S(x_i)$ in eq 1 is defined[15] as

$$S(x_i) = \frac{2}{x_i^2}\left(x_i - 1 + \left(\frac{h_i}{h_i + x_i}\right)^{h_i}\right) \quad (2)$$

where

$$x_i = \frac{q^2 N_{n,i} b_i^2}{6} \quad (3a)$$

and

$$h_i = \left(\frac{N_{w,i}}{N_{n,i}} - 1\right)^{-1} \quad (3b)$$

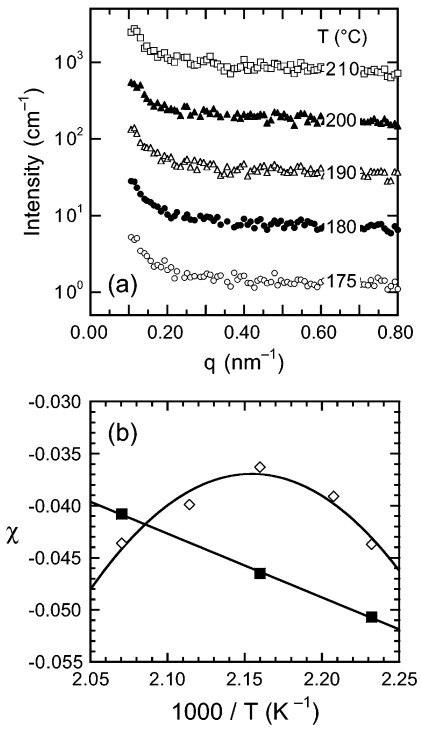

Figure 1. In (a), small-angle neutron scattering (SANS) patterns acquired from the 55/45 d_8-PMMA/PVDF blend at ambient pressure and five temperatures in the melt (in °C): 175 (○), 180 (●), 190 (△), 200 (▲), and 210 (□). The data sets are shifted vertically by a factor of 5× to facilitate examination. In (b), dependence of the Flory−Huggins χ interaction parameter extracted from SANS data as a function of reciprocal temperature at ambient pressure (◇) and 13.8 MPa of CO_2 (■). The solid lines denote regressed fits to quadratic and linear relationships, respectively.

In eq 3, b_i represents the statistical segment length of repeat unit i and $N_{w,i}$ is the weight-average degree of polymerization of polymer i.

The volume fractions utilized in eq 1 require the melt densities of PMMA and PVDF at the experimental temperatures. Polymer melt densities can be accurately estimated from a variety of equations of state developed for macromolecular systems. For this purpose, we elect to use the Hartmann−Haque[16] semiempirical equation of state, which can be written as

$$\tilde{p}\tilde{v}^5 = \tilde{T}^{3/2} - \ln \tilde{v} \quad (4)$$

where $\tilde{p} \equiv p/B_0$ (p corresponds to pressure), $\tilde{v} \equiv \hat{v}/\hat{v}_0$ ($\hat{v}$ is the specific volume), and $\tilde{T} \equiv T/T_0$ (T denotes absolute temperature). The values of B_0, $\hat{v}_0$, and T_0 are tabulated[15] for PMMA but must be estimated for molten PVDF using the correlations described by van Krevelen.[17] The normalizing parameters needed in eq 4, as well as the melt densities (ρ) predicted therefrom at ambient pressure, are listed in Table 1. Values of ρ calculated from the empirical Spencer−Gilmore[18] equation of state for PMMA are virtually identical (differing by less than 1.1%) to those provided in Table 1.

Fitting eq 1 to SANS patterns such as those displayed in Figure 1a yields χ as a function of temperature. This relationship is presented in Figure 1b for d_8-PMMA/PVDF blends with and without CO_2. In the absence of CO_2, χ is quadratically dependent on reciprocal temperature:

$$\chi = -4.76 + 4390/T - 1.02 \times 10^6/T^2 \quad (5)$$

Table 1. Values of the Parameters Used in the Hartmann−Haque[16] Semiempirical Equation of State (Eq 4) and Predicted Melt Densities

	T (°C)	PMMA	PVDF
B_0 (GPa)		3.84	3.6
$\hat{v}_0$ (cm^3/g)		0.757	0.569
T_0 (K)		1453	1170
ρ (g/cm^3)	175	1.11	1.39
	180	1.11	1.38
	190	1.10	1.37
	200	1.10	1.36
	210	1.09	1.35

According to the Flory−Huggins[19] equation of state, this functional relationship generally signifies that the blend exhibits both LCST and UCST behavior. However, since χ is always negative (indicating that the temperatures investigated are far from any critical point), a phase diagram cannot be generated[20] from eq 5. Instead, Figure 2 is provided as an illustration of the phase diagram based on critical temperatures previously reported[7,8,21,22] for various PMMA/PVDF blends. Within the context of this illustration, the UCST boundary inersects the composition-dependent $T_{g,mix}$ line generated from the Jenckel−Heusch[23] equation given by

$$T_{g,mix} = w_{PVDF}T_{g,PVDF} + w_{PMMA}T_{g,PMMA} + m(T_{g,PMMA} - T_{g,PVDF})w_{PVDF}w_{PMMA} \quad (6)$$

where w_j (j = PMMA or PVDF) represents the mass fraction of j and m is a constant set equal to 0.40. The glass transition temperatures of the neat homopolymers are 130 °C (d_8-PMMA) and −37 °C (PVDF), and $T_{g,mix}$ of the 55/45 d_8-PMMA/PVDF blend is 67 °C. Intersection of the UCST boundary with the $T_{g,mix}$ line is responsible for the observation that homogeneous PMMA/PVDF blends can be kinetically frozen-in at temperatures within the two-phase envelope.

Exposure of the blend to 13.8 MPa of CO_2 promotes a profound change in the effective $\chi(T)$ between d_8-PMMA and PVDF. Although we recognize that the ternary d_8-PMMA/PVDF/CO_2 system rigorously involves three pairwise-specific interaction parameters,[24] we elect to invoke a pseudo-binary approximation[25] for this system so that an effective $\chi(T)$ can be analyzed as a single parameter for comparative purposes. In the presence of CO_2 at 33 °C and 10 MPa, PMMA is reported[26] to swell by 22%, whereas amorphous PVDF is estimated[27] to swell by ∼10% at 75 °C and 15 MPa. While such swelling is indeed substantial, it is neglected in the present analysis of χ, since it has been found to have a relatively small effect on the value of χ extracted from small-angle scattering for this particular blend. Over the same temperature range used to determine $\chi(T)$ without CO_2 in Figure 1b, χ in the presence of CO_2 becomes linearly dependent on reciprocal temperature:

$$\chi = 8.61 \times 10^{-2} - 61.3/T \quad (7)$$

This relationship indicates that (i) the solvated blend exhibits evidence of only LCST behavior and (ii) the temperature range investigated is closer to a critical point. The latter point implies that the LCST boundary is lowered by the presence of CO_2, which is consistent with our observations of poly(ethyl methacrylate)/PVDF blends. We refrain from using eq 7 to generate the corresponding phase boundary predicted by the Flory-Huggins[19] equation of state, since this formalism does not include compressibility effects. In related efforts,

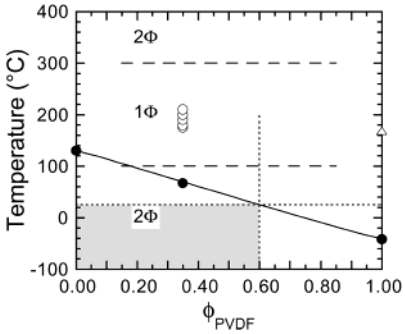

Figure 2. An illustrative phase diagram of the d_8-PMMA/PVDF system derived from the thermal characteristics of the present blend, in conjunction with critical temperatures (dashed lines) approximated by values previously reported.[7,8,21,22] Homogeneous and heterogeneous regions are labeled as 1Φ and 2Φ, respectively, and the temperatures at which the data in Figure 1a were collected are denoted by (○). The melting point of PVDF (△) and the glass transition temperatures of d_8-PMMA, PVDF, and the 55/45 d_8-PMMA/PVDF blend without CO_2 are also shown (●), as are predictions of $T_{g,mix}(\phi_{PVDF})$ (solid line) generated from the Jenckel−Heusch[23] equation (eq 6). The intersecting (dotted) lines identify the blend composition (∼60 vol % PVDF) at which $T_{g,mix}$ coincides with ambient temperature (25 °C), thereby indicating the range of ϕ_{PVDF} over which a miscible blend could be kinetically frozen-in within the UCST envelope (shaded).

RamachandraRao and Watkins[28] have shown that high-pressure CO_2 can significantly lower the phase boundary of the LCST polystyrene/poly(vinyl methyl ether) (PS/PVME) blend. Their reported reduction in blend miscibility is attributed to free volume, rather than enthalpic, effects, which may be crucial in distinguishing PS/PVME blends from PMMA/PVDF blends in terms of their thermodynamic response to high-pressure CO_2. Recall that specific intermolecular interactions are responsible for PMMA/PVDF blends exhibiting LCST behavior at temperatures above T_m. In the presence of high-pressure CO_2, these interactions, as well as those that are repulsive in nature, are screened, but to different extents. The overall degree to which such molecular screening occurs dictates the accompanying shift in the phase boundary. In the case of PS/PVME blends, CO_2 amplifies the free volume disparity of the constituent polymers and promotes immiscibility at elevated temperatures. Since the phase behavior of polymer blends in the presence of CO_2 is becoming increasingly important, we hasten to add that CO_2 can likewise serve to either improve or reduce the miscibility of UCST blends composed of PS/polyisoprene[29] or poly(dimethylsiloxane)/poly(ethylmethylsiloxane),[30] respectively.

Figure 3a displays SANS patterns acquired from the 55/45 d_8-PMMA/PVDF blend in the solid state at 25 °C and several different CO_2 pressures. Using densities for amorphous PMMA and PVDF (1.10 and 1.68 g/cm^3, respectively[31]) to determine the blend volume fraction and fitting eq 1 to these four scattering patterns yields the χ values provided in Figure 3b. An initial increase in CO_2 pressure from 0 to 6.89 MPa promotes a sharp increase in χ from -8.85×10^{-2} to -3.28×10^{-3}. At higher pressures, the change in χ becomes slight, suggesting that χ does not, within experimental uncertainty, deviate much from zero under these conditions. This trend is generally similar to that discerned from small-angle X-ray scattering (SAXS) of miscible PMMA/PVDF blends in the presence of high-pressure CO_2, although we note that our SAXS analysis reveals that

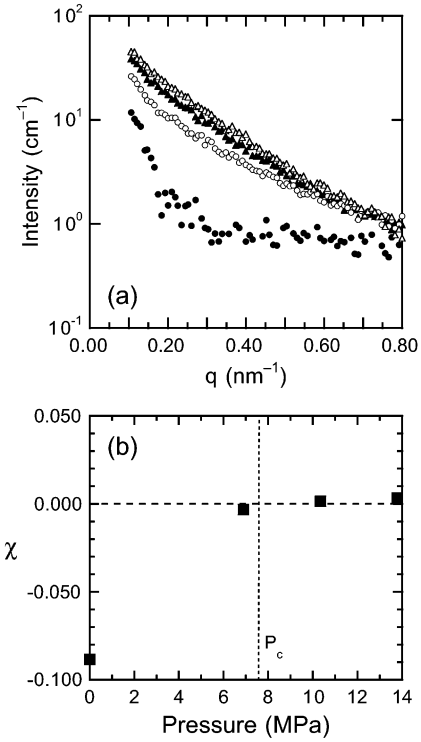

Figure 3. In (a), SANS patterns collected from the 55/45 d_8-PMMA/PVDF blend at 25 °C in the solid state and four CO_2 pressures (in MPa): 0 (●), 6.89 (○), 10.3 (▲), and 13.8 (△). The data sets are not shifted. In (b), dependence of the Flory–Huggins χ interaction parameter extracted from the SANS data in (a) on CO_2 pressure at 25 °C. The critical pressure (P_c) of CO_2 is displayed as the dotted vertical line.

the ultimate increase in χ is preceded by little variation in χ.[11] While we cannot discount the possibility that χ increases measurably beyond zero at higher CO_2 pressures, no evidence presently exists to confirm such variation (to endothermic mixing). The limiting behavior of χ apparent in Figure 3b implies that the PMMA and PVDF components become chemically indistinguishable, forming an "ideal" or Θ blend,[32] which is consistent with the CO_2-induced elimination of the UCST phase boundary. Another important characteristic of Figure 3a is the abrupt increase in scattering intensity coincident with increasing the CO_2 pressure from 0 to 6.89 MPa. This feature most likely reflects the onset of PVDF crystallization. As discussed by Papavoine et al.[10] and Wellscheid et al.,[22] crystallization of PVDF in miscible blends with acrylics routinely ensues upon isothermal annealing at temperatures above $T_{g,mix}$ and below T_m due to increased molecular mobility in the melt.

Similarly, Chiou and Paul[33] and Briscoe et al.[34] have shown that CO_2 can promote PVDF crystallization in miscible PMMA/PVDF blends and neat PVDF, respectively. In the case of the blends, PVDF crystallization can occur near ambient temperature due to extensive plasticization[35] of the blend and a corresponding reduction in $T_{g,mix}$. Enhanced molecular mobility is therefore achieved through the addition of high-pressure CO_2 as a diluent. The DSC thermograms presented in Figure 4 confirm that the 55/45 d_8-PMMA/PVDF blend initially exhibits a $T_{g,mix}$ of 67 °C (trace a). Upon exposure to 13.8 MPa at 25 °C (trace b) or 180 °C and cooled (trace d), the blend exhibits a melting endotherm whose peak is centered at 150 °C, which is noticeably lower than T_m of the neat PVDF at 168 °C (trace f). This reduction in T_m reveals that the PVDF crystals are not as well

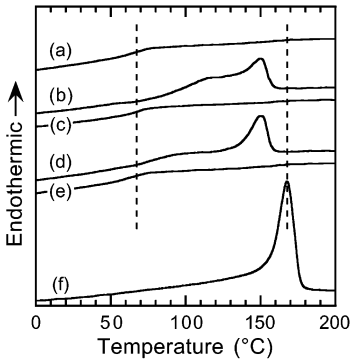

Figure 4. Differential scanning calorimetry (DSC) thermograms of the 55/45 d_8-PMMA/PVDF blend before (a) and after (b, d) exposure to 13.8 MPa of CO_2, as well as the neat PVDF (f). Specimens have been exposed to CO_2 in the solid state at ambient temperature (b) and in the melt at 180 °C and subsequently cooled to ambient temperature under CO_2 pressure (d). Second heating cycles for traces (b) and (d) are displayed as (c) and (e), respectively. The traces are shifted vertically to facilitate examination, and the dashed vertical lines identify $T_{g,mix}$ of the blend (67 °C) and T_m of the neat PVDF (168 °C). The heating rate is constant at 10 °C/min.

ordered as in neat PVDF, which is consistent with transmission electron microscopy (TEM) results reported elsewhere.[11] Moreover, the degree of crystallinity of the neat PVDF is estimated from the heat of melting (Δh_m) to be ~39%, whereas that of PVDF in the specimen displayed in trace d is less (~30%). Thermal cycling of the specimens exposed to high-pressure CO_2 in the solid state (trace b) or in the melt and then cooled under CO_2 pressure (trace d) eliminates the melting endotherms (see traces c and e, respectively), indicating that CO_2-induced crystallization in PMMA/PVDF blends is thermally reversible.

Conclusions. This study explores the phase behavior of PMMA/PVDF blends alone and in the presence of high-pressure CO_2. In the absence of CO_2, χ for this blend is quadratic in reciprocal temperature and always negative, indicating that it cannot be used to construct a phase diagram. In the presence of high-pressure CO_2, the dependence of χ on reciprocal temperature becomes linear, confirming the existence of LCST behavior at elevated temperatures and implying a reduction in the LCST phase boundary. At ambient temperature, the addition of CO_2 at 6.89 MPa promotes an increase in χ up to about $\chi \approx 0$. Increasing the CO_2 pressure above 6.89 MPa further increases χ, but only to a relatively small extent. The initial increase in χ is accompanied by an increase in scattering intensity, which is attributed to PVDF crystallization, as evidenced by thermal calorimetry. This study confirms that high-pressure CO_2 can not only have a profound effect on the phase behavior of polymer blends but also open new polymer process, property, or morphology windows.

Acknowledgment. This study was supported by the Kenan Center for the Utilization of Carbon Dioxide in Manufacturing and the STC Program of the National Science Foundation under Agreement CHE-9876674. The research performed at Oak Ridge was supported, in part, by the Division of Materials Sciences, under Contract DE-AC05-00OR22725 with the Oak Ridge National Laboratory, managed by UT-Battelle, LLC. We thank C. A. Eckert for a helpful discussion.

References and Notes

(1) Brandrup, J., Immergut, E. H., Grulke, E. A., Eds. *Polymer Handbook*, 4th ed.; Wiley & Sons: New York, 1999; p V-49.
(2) Brydson, J. A., Ed. *Plastics Materials*, 6th ed.; Butterworth-Heinemann: Oxford, 1995; p 390.
(3) Linares, A.; Acosta, J. L. *Eur. Polym. J.* **1997**, *33*, 467.
(4) Leonard, C.; Halary, J. L.; Monnerie, L. *Polymer* **1985**, *26*, 1507.
(5) Moskala, E. J.; Varnell, D. F.; Coleman, M. M. *Polymer* **1985**, *26*, 228.
(6) Siripurapu, S.; Gay, Y. J.; Royer, J. R.; DeSimone, J. M.; Spontak, R. J.; Khan, S. A. *Polymer* **2002**, *43*, 5511.
(7) Saito, H.; Fujita, Y.; Inoue, T. *Polym. J.* **1987**, *19*, 405. Tomura, H.; Saito, H.; Inoue, T. *Macromolecules* **1992**, *25*, 1611.
(8) Shimada, S.; Hori, Y.; Kashiwabara, H. *Macromolecules* **1988**, *21*, 3454.
(9) Grinsted, R. A.; Koenig, J. L. *J. Polym. Sci., Part B: Polym. Phys.* **1990**, *28*, 177.
(10) Papavoine, C. H. M.; Mass, W. E. J. R.; Veeman, W. S.; Werumeus Burning, G. H.; Vankan, J. M. J. *Macromolecules* **1993**, *26*, 6611.
(11) Walker, T. A.; Melnichenko, Y. B.; Wignall, G. D.; Lin, J. S.; Spontak, R. J. Manuscript in preparation.
(12) Ribbe, A. E.; Hashimoto, T. *Macromolecules* **2000**, *33*, 7827.
(13) Wignall, G. D.; Bates, F. S. *J. Appl. Crystallogr.* **1987**, *20*, 28.
(14) de Gennes, P. G. *Scaling Concepts in Polymer Physics*; Cornell University Press: Ithaca, NY, 1979.
(15) Sakurai, S.; Hasegawa, H.; Hashimoto, T.; Hargis, I. G.; Aggarwal, S. L.; Han, C. C. *Macromolecules* **1990**, *23*, 451.
(16) Hartmann, B.; Haque, M. A. *J. Appl. Polym. Sci.* **1985**, *30*, 1553.
(17) van Krevelen, D. W. *Properties of Polymers*, 3rd ed.; Elsevier: Amsterdam, 1997.
(18) Spencer, R. S.; Gilmore, G. D. *J. Appl. Phys.* **1949**, *20*, 502; **1950**, *21*, 523. McCrum, N. G.; Buckley, C. P.; Bucknall, C. B. *Principles of Polymer Engineering*, 2nd ed.; Oxford University Press: Oxford, 1997; p 336.
(19) Flory, P. J. *Principles of Polymer Chemistry*; Cornell University Press: Ithaca, NY, 1953.
(20) Balsara, N. P. In *Physical Properties of Polymers Handbook*; Mark, J. E., Ed.; AIP Press: Woodbury, NY, 1996; Chapter 19.
(21) Bernstein, R. E.; Cruz, C. A.; Paul, D. R.; Barlow, J. W. *Macromolecules* **1977**, *10*, 681.
(22) Wellscheid, R.; Wüst, J.; Jungnickel, B.-J. *J. Polym. Sci., Part B: Polym. Phys.* **1996**, *34*, 267.
(23) Jenckel, E.; Heusch, R. *Kolloid Z. Z. Polym.* **1953**, *130*, 89.
(24) Benmouna, M.; Hammouda, B. *Prog. Polym. Sci.* **1997**, *22*, 49.
(25) Lodge, T. P.; Pan, C.; Jin, X.; Liu, Z.; Zhao, J.; Maurer, W. W.; Bates, F. S. *J. Polym. Sci., Part B: Polym. Phys.* **1995**, *33*, 2289.
(26) Wissinger, R. G.; Paulaitis, M. E. *J. Polym. Sci., Part B: Polym. Phys.* **1987**, *25*, 2497.
(27) Kennedy, K. A. Ph.D. Dissertation, North Carolina State University, 2003.
(28) RamachandraRao, V. S.; Watkins, J. J. *Macromolecules* **2000**, *33*, 5143.
(29) Walker, T. A.; Raghavan, S. R.; Royer, J. R.; Smith, S. D.; Wignall, G. D.; Melnichenko, Y.; Khan, S. A.; Spontak, R. J. *J. Phys. Chem. B* **1999**, *103*, 5472.
(30) Walker, T. A.; Colina, C. M.; Gubbins, K. E.; Spontak, R. J. Manuscript in preparation.
(31) Scheinbeim, J. I. In *Polymer Data Handbook*; Mark, J. E., Ed.; Oxford University Press: Oxford, 1999; p 950.
(32) Melnichenko, Y. B.; Wignall, G. D.; Schwahn, D. *Phys. Rev. E* **2002**, *65*, 061802.
(33) Chiou, J. S.; Paul, D. R. *J. Appl. Polym. Sci.* **1986**, *32*, 2897.
(34) Briscoe, B. J.; Lorge, O.; Wajs, A.; Dang, P. *J. Polym. Sci., Part B: Polym. Phys.* **1998**, *36*, 2435.
(35) Chiou, J. S.; Barlow, J. W.; Paul, D. R. *J. Appl. Polym. Sci.* **1985**, *30*, 2633.

MA030103C